PHYSICAL REVIEW A VOLUME 28, NUMBER 6 DECEMBER 1983

Filamentation and modulational instabilities of an upper hybrid laser radiation in a hot collisionless magnetoplasma

Md. Salimullah
Department of Physics, Jahangirnagar University, Savar, Dhaka, Bangladesh
(Received 15 October 1982)

This paper presents a rigorous theoretical investigation of the filamentation and modulational instabilities of an upper hybrid laser radiation in a hot, collisionless and homogeneous plasma in the presence of the self-generated dc magnetic field of the order of a few megagauss. Fluid equations have been employed to find the nonlinear response of electrons. The low-frequency nonlinearity arises through the ponderomotive force on electrons, whereas the high-frequency nonlinearity arises through the current densities associated with the scattered sidebands. It is observed that the growth rate of the filamentation instability decreases with increasing magnetic field, while the growth rate of the modulational instability increases with increasing magnetic field. Furthermore, the growth rate of the filamentation instability is higher by about one order of magnitude than that of the modulational instability for the same set of plasma parameters.

I. INTRODUCTION

In the laser-pellet fusion plasmas the self-generated magnetic field of the order of few megagauss is generated due to a variety of reasons.[1-9] Such high magnetic fields must influence drastically the absorption processes of the laser beams and the transport properties of the plasma.[10,11] Again, since the powers employed in the laser-pellet fusion experiments are very high, the nonlinear effects, e.g., paramagnetic instabilities, profile modification, etc., should become important.[12-17] The earlier literature on parametric instabilities of laser radiation is, however, mainly restricted to the unmagnetized or weakly magnetized plasmas. Therefore, the effects of the self-generated high dc magnetic field on the various parametric processes must be considered in detail.

The absorption of the laser beam in a plasma is dependent upon the scattering processes in the underdense region since the resonance absorption is one of the major processes by which the laser energy must reach the critical density layer to be effectively absorbed.[18,19] Therefore, the scattering processes in a magnetized plasma play a relevant part in the theoretical understanding of the beam-target fusion experiments. Shukla *et al.*[20] have studied the nonlinear sidescattering of an upper hybrid laser radiation by upper hybrid and lower hybrid waves in an inhomogeneous plasma. Larson[19] and Johnston and Kaufman[21] have derived general expressions for the coupling coefficients of the three-wave decay of electromagnetic waves in a magnetized plasma. Using the fluid model Grebogi and Liu[22] have investigated the enhanced Brillouin and Raman scattering of extraordinary laser radiation in a plane perpendicular to the self-generated magnetic field by upper hybrid and lower hybrid modes in a plasma. Porkolab and Goldman[23] have studied the soliton and oscillating two-stream instability of upper hybrid electrostatic waves in a plasma. Tripathi and Sharma[22] have also studied the decay instability of the upper hybrid laser radiation into various channels of decay by using fluid and kinetic descriptions. In all these studies very-short-wavelength perturbations have been considered, where $b=k^2\rho_e^2/2\gg 1$ (k is the propagation vector of the perturbation and ρ_e is the electron Larmor radius) and only one scattered sideband is important. But for long-wavelength perturbations, both the Stokes and anti-Stokes components of the scattered waves should be important. Moreover, depending upon the direction of propagation of the perturbations, the incident beam may suffer filamentation and modulational instabilities.[16,24-29] To the best knowledge of the author no work seems to have been reported in the literature on the filamentation and modulational instabilities of the upper hybrid laser radiation, where the self-generated magnetic field might play a vital role.

In this paper we have given a rigorous theory for the filamentation and modulational instabilities of a high-power upper hybrid laser beam in a homogeneous plasma in the presence of a high magnetic field. We consider the long-wavelength perturbations which may be present in the plasma due to the presence of an ion acoustic mode or some other reasons. The nonlinearity in our analysis arises through the ponderomotive force on electrons.

In Sec. II we have derived the nonlinear dispersion relation for the low-frequency electrostatic perturbation when an upper hybrid laser radiation propagates in a direction perpendicular to the self-generated dc magnetic field and polarized in a plane perpendicular to the magnetic field. The low-frequency nonlinear response of electrons in the plasma has been obtained by the use of the fluid equations which are sufficiently valid for the long-wavelength perturbations. The dispersion relation is then solved to obtain the growth rates of the decay waves for the filamentation and modulational instabilities in Sec. III. Some numerical estimates of the growth rates are also given in Sec. III. Finally, a brief discussion of the results is presented in Sec. IV.

II. NONLINEAR DISPERSION RELATION

We consider the propagation of an upper hybrid laser radiation (pump) in a homogeneous plasma along the x axis with its electric vector polarized in a plane perpendicular to the self-generated magnetic field $\vec{B}_s$ along the z direction:

$$\vec{E}_0=\vec{E}'_0\exp[-i(\omega_0 t-k_0 x)] , \tag{1}$$

where

$$E_{0x}=i\alpha E_{0y} , \tag{2}$$

$$\alpha=-\frac{\omega_c}{\omega_0}\frac{\omega_p^2}{\omega_0^2-\omega_{UH}^2} , \tag{3}$$

$$k_0=\frac{\omega_0}{c}\left[1-\frac{\omega_p^2}{\omega_0^2}\frac{\omega_0^2-\omega_p^2}{\omega_0^2-\omega_{UH}^2}\right]^{1/2} , \tag{4}$$

$$\omega_{UH}^2=\omega_p^2+\omega_c^2 . \tag{5}$$

Here, $\omega_p=(4\pi n_0^0 e^2/m)^{1/2}$ and $\omega_c=eB_s/mc$ are the electron plasma frequency and electron cyclotron frequency; $-e$, m, n_0^0, and c are electronic charge, mass, unperturbed electron density, and the velocity of light in vacuum, respectively. The incident laser radiation possesses an oscillatory magnetic field, $\vec{B}_0=c\vec{k}_0\times\vec{E}_0/\omega_0$ and gives rise to an oscillatory drift velocity of electrons,

$$\vec{V}_{0\perp}=\frac{e}{m}\frac{\vec{E}_{0\perp}\times\vec{\omega}_c+i\omega_0\vec{E}_{0\perp}}{\omega_c^2-\omega_0^2} , \tag{5'}$$

where the symbol $\perp$ denotes the component of the corresponding vector transverse to the self-generated dc magnetic field $\vec{B}_s\|\hat{z}$.

The oscillatory drift velocity of electrons due to the pump wave and the oscillatory magnetic field of the pump wave interact parametrically with the low-frequency mode $(\omega,\vec{k})$ in the plasma and produce two high-frequency sidebands $(\omega_{1,2}=\omega\mp\omega_0,\vec{k}_{1,2}=\vec{k}\mp\vec{k}_0)$. These generated sidebands, in turn, interact with the pump wave to produce a nonlinear low-frequency ponderomotive force which amplifies and drives the perturbation $(\omega,\vec{k})$. Thus, we are considering the parametric decay of the pump wave into a low-frequency perturbation and two high-frequency sidebands. Since we consider the long-wavelength perturbation, both the sidebands must be taken into account.[16]

The total response of electrons to this four-wave parametric process is governed by the following fluid equations:

(i) the momentum-balance equation

$$\frac{\partial\vec{V}}{\partial t}=-\frac{e\vec{E}}{m}-(\vec{V}\cdot\vec{\nabla})\vec{V}-\frac{e}{mc}(\vec{V}\times\vec{B})-(\vec{V}\times\vec{\omega}_c)-\frac{V_e^2}{n_0^0}\vec{\nabla}n , \tag{6}$$

(ii) the equation of continuity

$$\frac{\partial n}{\partial t}+\vec{\nabla}\cdot(n\vec{V})=0 , \tag{7}$$

where $V_e=(2k_BT_e/m)^{1/2}$ is the electron thermal speed, n_0^0 is the equilibrium electron density, k_B is the Boltzmann constant, and T_e is the temperature of electrons in the plasma. The second and third terms on the right-hand side of Eq. (6) constitute the ponderomotive force which is the major nonlinear source in the low-frequency response. For the high-frequency response the nonlinearity arises through the equation of continuity, Eq. (7). The linear velocity components for the high-frequency sidebands are obtained by solving Eqs. (6) and (7) as

$$\vec{V}_{1\perp,2\perp}=\frac{e}{m}\frac{\vec{E}_{1\perp,2\perp}\times\vec{\omega}_c+i\omega_{1,2}\vec{E}_{1\perp,2\perp}}{\omega_c^2-\omega_{1,2}^2} , \tag{8}$$

$$V_{1z,2z}=\frac{eE_{1z,2z}}{mi(\omega_{1,2}-k_{1,2}^2V_e^2/\omega_{1,2})} . \tag{9}$$

Now, without loss of any generality we assume that the scattered electromagnetic sidebands $(\omega_1,\vec{k}_1)$ and $(\omega_2,\vec{k}_2)$ propagate in the XZ plane, so that, k_{1y}, k_{2y}, $k_y=0$. Also, the low-frequency perturbation is assumed to be purely electrostatic $(\vec{E}=-\vec{\nabla}\phi)$. Using Eqs. (6) and (7) and retaining all the components of the ponderomotive force, we obtain the following expression for the nonlinear density perturbation associated with the low-frequency electrostatic mode in the plasma:

$$n(\omega,\vec{k})=\frac{\chi_e k^2}{4\pi e}\phi-\frac{e^2n_0^0}{2m^2\omega(\omega_c^2-\omega_0^2)}(E_{0y}X+E_{0y}^*Y) , \tag{10}$$

where

$$\chi_e=\frac{i\omega_p^2}{k^2\omega}\left[\frac{k_x^2 f}{\omega_c^2+f^2}+\frac{k_z^2}{f}\right] \tag{11}$$

is the electronic susceptibility and

$$X=\left[\frac{ifk_x}{\omega_c^2+f^2}\left[\frac{\omega_c}{\omega_0}k_0+\frac{\omega_1(\omega_c-\alpha\omega_0)}{\omega_c^2-\omega_0^2}(k_0+k_{1x})\right]-\frac{i\omega_c k_x}{\omega_c^2+f^2}\left[\frac{\omega_1}{\omega_0}k_0+\frac{\omega_c(\omega_c-\alpha\omega_0)}{\omega_c^2-\omega_0^2}k_{1x}+\frac{\omega_1(\omega_0-\alpha\omega_c)}{\omega_c^2-\omega_0^2}k_0\right]-\frac{\omega_c-\alpha\omega_0}{f\omega_1}k_zk_{1z}\right]E_{1x}$$
$$+\left[\frac{fk_x}{\omega_c^2+f^2}\left[\frac{\omega_1}{\omega_0}k_0+\frac{\omega_0-\alpha\omega_c}{\omega_1}k_{1x}+\frac{\omega_c(\omega_c-\alpha\omega_0)}{\omega_c^2-\omega_0^2}(k_0+k_{1x})\right]\right.$$

$$-\frac{\omega_c k_x}{\omega_c^2+f^2}\left[\frac{\omega_c}{\omega_0}k_0+\frac{\omega_c(\omega_0-\alpha\omega_c)}{\omega_c^2-\omega_0^2}k_0+\frac{\omega_c^2(\omega_c-\alpha\omega_0)}{\omega_1(\omega_c^2-\omega_0^2)}k_{1x}\right]-\frac{i(\omega_0-\alpha\omega_c)}{f\omega_1}k_z k_{1z}\Bigg]E_{1y}$$

$$-\left[\frac{\omega_c-\alpha\omega_0}{f}\left[\frac{1}{\omega_1-k_1^2V_e^2/\omega_1}-\frac{1}{\omega_1}\right]k_z k_{1x}\right]E_{1z}\ , \tag{12}$$

$$Y=\Bigg[\frac{ifk_x}{\omega_c^2+f^2}\left[\frac{\omega_c}{\omega_0}k_0-\frac{\omega_2(\omega_c-\alpha\omega_0)}{\omega_c^2-\omega_0^2}(k_0-k_{2x})\right]$$

$$-\frac{i\omega_c k_x}{\omega_c^2+f^2}\left[\frac{\omega_2}{\omega_0}k_0+\frac{\omega_2(\omega_0-\alpha\omega_c)}{\omega_c^2-\omega_0^2}k_0+\frac{\omega_c(\omega_c-\alpha\omega_0)}{\omega_c^2-\omega_0^2}k_{2x}\right]+\frac{\omega_c-\alpha\omega_0}{f\omega_2}k_z k_{2z}\Bigg]E_{2x}$$

$$+\Bigg[\frac{fk_x}{\omega_c^2+f^2}\left[\frac{\omega_2 k_0}{\omega_0}-\frac{(\omega_0-\alpha\omega_c)}{\omega_2}k_{2x}-\frac{\omega_c(\omega_c-\alpha\omega_0)}{\omega_c^2-\omega_0^2}(k_0-k_{2x})\right]$$

$$-\frac{\omega_c k_x}{\omega_c^2+f^2}\left[\frac{\omega_c}{\omega_0}k_0+\frac{\omega_c(\omega_0-\alpha\omega_c)}{\omega_c^2-\omega_0^2}k_0+\frac{\omega_c^2(\omega_c-\alpha\omega_0)}{\omega_2(\omega_c^2-\omega_0^2)}k_{2x}\right]-\frac{i(\omega_0-\alpha\omega_c)}{f\omega_2}k_z k_{2z}\Bigg]E_{2y}$$

$$+\left[\frac{\omega_c-\alpha\omega_0}{f}\left[\frac{1}{\omega_2-k_2^2V_e^2/\omega_2}-\frac{1}{\omega_2}\right]k_z k_{2x}\right]E_{2z}\ , \tag{13}$$

$$f=-i\omega+ik^2V_e^2/\omega\ . \tag{14}$$

The nonlinear current densities at the high-frequency sidebands are given by

$$\vec{J}_1(\omega_1,\vec{k}_1)=-n_0^0 e\left[\frac{e(\vec{E}_{1\perp}\times\vec{\omega}_c+i\omega_1\vec{E}_{1\perp})}{m(\omega_c^2-\omega_1^2)}+\hat{z}\frac{eE_{1z}}{mi(\omega_1-k_1^2V_e^2/\omega_1)}\right]-\frac{en(\omega,\vec{k})}{2}\vec{V}_0^*\ , \tag{15}$$

$$\vec{J}_2(\omega_2,\vec{k}_2)=-n_0^0 e\left[\frac{e(\vec{E}_{2\perp}\times\vec{\omega}_c+i\omega_2\vec{E}_{2\perp})}{m(\omega_c^2-\omega_2^2)}+\hat{z}\frac{eE_{2z}}{mi(\omega_2-k_2^2V_e^2/\omega_2)}\right]-\tfrac{1}{2}n(\omega,\vec{k})e\vec{V}_0\ . \tag{16}$$

Using Eq. (10) in the Poisson's equation and Eqs. (15) and (16) in the wave equations for the high-frequency sidebands, we obtain

$$\epsilon\phi=-4\pi e n^{\rm NL}/k^2\ , \tag{17}$$

$$\overleftrightarrow{D}_1\cdot\vec{E}_1=\alpha_1[\hat{x}(\omega_c-\alpha\omega_0)-\hat{y}i(\omega_0-\alpha\omega_c)]\ , \tag{18}$$

$$\overleftrightarrow{D}_2\cdot\vec{E}_2=\alpha_2[\hat{x}(\omega_c-\alpha\omega_0)+\hat{y}i(\omega_0-\alpha\omega_c)]\ , \tag{19}$$

where

$$\epsilon=1+\chi_e\ , \tag{20}$$

$$\overleftrightarrow{D}_{1,2}=k_{1,2}^2\overleftrightarrow{I}-\vec{k}_{1,2}\vec{k}_{1,2}-\frac{\omega_{1,2}^2}{c^2}\overleftrightarrow{\epsilon}_{1,2}\ , \tag{21}$$

$$\alpha_1=-\frac{i\omega_1\chi_e k^2\phi}{2c^2}\frac{eE_{0y}^*}{m(\omega_c^2-\omega_0^2)}\ , \tag{22}$$

$$\alpha_2=-\frac{i\omega_2\chi_e k^2\phi}{2c^2}\frac{eE_{0y}}{m(\omega_c^2-\omega_0^2)}\ , \tag{23}$$

and $\overleftrightarrow{I}$ is the unity tensor of rank 2 and $n^{\rm NL}$ is the nonlinear part of $n(\omega,\vec{k})$. The linear part of $n(\omega,\vec{k})$ has been neglected in Eq. (17) and nonlinear part of $n(\omega,\vec{k})$ has been neglected in Eqs. (18) and (19). In Eq. (17) ϵ is the linear dielectric function of the low-frequency electrostatic perturbation. $\overleftrightarrow{\epsilon}_{1,2}$ in Eq. (21) are the linear dielectric tensors for the high-frequency sidebands[30]:

$$\overleftrightarrow{\epsilon}_{1,2}=\begin{bmatrix} 1-\dfrac{\omega_p^2}{\omega_{1,2}^2-\omega_c^2} & \dfrac{i\omega_p^2}{\omega_{1,2}^2-\omega_c^2}\dfrac{\omega_c}{\omega_{1,2}} & 0 \\ -\dfrac{i\omega_p^2}{\omega_{1,2}^2-\omega_c^2}\dfrac{\omega_c}{\omega_{1,2}} & 1-\dfrac{\omega_p^2}{\omega_{1,2}^2-\omega_c^2} & 0 \\ 0 & 0 & 1-\dfrac{\omega_p^2}{\omega_{1,2}^2} \end{bmatrix} . \tag{24}$$

Eliminating ϕ, $\vec{E}_1$, and $\vec{E}_2$ from Eqs. (17)—(19) we obtain the nonlinear dispersion relation for the low-frequency perturbation, after a little simplification, as

$$\epsilon=\frac{\mu_1}{|\overleftrightarrow{D}_1|}+\frac{\mu_2}{|\overleftrightarrow{D}_2|} , \tag{25}$$

where

$$\begin{aligned}\mu_1=&-\frac{|V_{0y}/c|^2\omega_p^2\omega_1\chi_e}{4\omega(\omega_c+\omega_0)^2}\\ &\times\Bigg[\left[k_{1x}^2-\frac{\omega_1^2}{c^2}\left[1-\frac{\omega_p^2}{\omega_1^2}\right]\right]\left\{(\omega_c-\alpha\omega_0)\left[k_1^2-\frac{\omega_1^2}{c^2}\left[1-\frac{\omega_p^2}{\omega_1^2-\omega_c^2}\right]\right]+(\omega_0-\alpha\omega_c)\left[\frac{\omega_1^2}{c^2}\left[\frac{\omega_p^2}{\omega_1^2-\omega_c^2}\frac{\omega_c}{\omega_1}\right]\right]\right\}\\ &\quad\times\left[\frac{-fk_x}{\omega_c^2+f^2}\left[\frac{\omega_c}{\omega_0}k_0+\frac{\omega_1(\omega_c-\alpha\omega_0)}{\omega_c^2-\omega_0^2}(k_0+k_{1x})\right]\right.\\ &\quad\quad\left.+\frac{\omega_c k_x}{\omega_c^2+f^2}\left[\frac{\omega_1}{\omega_0}k_0+\frac{\omega_1(\omega_0-\alpha\omega_c)}{\omega_c^2-\omega_0^2}k_0+\frac{\omega_c(\omega_c-\alpha\omega_0)}{\omega_c^2-\omega_0^2}k_{1x}\right]-\frac{i(\omega_c-\alpha\omega_0)}{f\omega_1}k_zk_{1z}\right]\\ &\quad+\left\{(\omega_c-\alpha\omega_0)\left[\frac{\omega_1^2}{c^2}\left[\frac{\omega_p^2}{\omega_1^2-\omega_c^2}\frac{\omega_c}{\omega_1}\right]\right]\left[k_{1x}^2-\frac{\omega_1^2}{c^2}\left[1-\frac{\omega_p^2}{\omega_1^2}\right]\right]\right.\\ &\quad\quad\left.+(\omega_0-\alpha\omega_c)\left\{\left[k_{1x}^2-\frac{\omega_1^2}{c^2}\left[1-\frac{\omega_p^2}{\omega_1^2}\right]\right]\left[k_{1z}^2-\frac{\omega_1^2}{c^2}\left[1-\frac{\omega_p^2}{\omega_1^2-\omega_c^2}\right]\right]-k_{1x}^2k_{1z}^2\right\}\right\}\\ &\quad\times\left[\frac{fk_x}{\omega_c^2+f^2}\left[\frac{\omega_1}{\omega_0}k_0+\frac{\omega_0-\alpha\omega_c}{\omega_1}k_{1x}+\frac{\omega_c(\omega_c-\alpha\omega_0)}{\omega_c^2-\omega_0^2}(k_0+k_{1x})\right]\right.\\ &\quad\quad\left.-\frac{\omega_c k_x}{\omega_c^2+f^2}\left[\frac{\omega_c}{\omega_0}k_0+\frac{\omega_c(\omega_0-\alpha\omega_c)}{\omega_c^2-\omega_0^2}k_0+\frac{\omega_c^2(\omega_c-\alpha\omega_0)}{\omega_1(\omega_c^2-\omega_0^2)}k_{1x}\right]-\frac{i(\omega_0-\alpha\omega_c)}{\omega_1 f}k_zk_{1z}\right]\\ &\quad+k_{1x}k_{1z}\left\{(\omega_c-\alpha\omega_0)\left[k_1^2-\frac{\omega_1^2}{c^2}\left[1-\frac{\omega_p^2}{\omega_1^2-\omega_c^2}\right]\right]+(\omega_0-\alpha\omega_c)\left[\frac{\omega_1^2}{c^2}\left[\frac{\omega_p^2}{\omega_1^2-\omega_c^2}\frac{\omega_c}{\omega_1}\right]\right]\right\}\\ &\quad\times\left[-\frac{i(\omega_c-\alpha\omega_0)}{f}\left[\frac{1}{\omega_1-k_1^2V_e^2/\omega_1}-\frac{1}{\omega_1}\right]k_zk_{1x}\right]\Bigg] ,\end{aligned} \tag{26}$$

$$\begin{aligned}\mu_2=&-\frac{|V_{0y}/c|^2\omega_p^2\omega_2\chi_e}{4\omega(\omega_c+\omega_0)^2}\\ &\times\Bigg[\left[k_{2x}^2-\frac{\omega_2^2}{c^2}\left[1-\frac{\omega_p^2}{\omega_2^2}\right]\right]\left\{(\omega_c-\alpha\omega_0)\left[k_2^2-\frac{\omega_2^2}{c^2}\left[1-\frac{\omega_p^2}{\omega_2^2-\omega_c^2}\right]\right]-(\omega_0-\alpha\omega_c)\left[\frac{\omega_2^2}{c^2}\left[\frac{\omega_p^2}{\omega_2^2-\omega_c^2}\frac{\omega_c}{\omega_2}\right]\right]\right\}\\ &\quad\times\left[\frac{-fk_x}{\omega_c^2+f^2}\left[\frac{\omega_c}{\omega_0}k_0-\frac{\omega_2(\omega_c-\alpha\omega_0)}{\omega_c^2-\omega_0^2}(k_0-k_{2x})\right]\right.\\ &\quad\quad\left.+\frac{\omega_c k_x}{\omega_c^2+f^2}\left[\frac{\omega_2}{\omega_0}k_0+\frac{\omega_2(\omega_0-\alpha\omega_c)}{\omega_c^2-\omega_0^2}k_0+\frac{\omega_c(\omega_c-\alpha\omega_0)}{\omega_c^2-\omega_0^2}k_{2x}\right]+\frac{i(\omega_c-\alpha\omega_0)}{f\omega_2}k_zk_{2z}\right]\end{aligned}$$

$$+\left[(\omega_c-\alpha\omega_0)\left[\frac{\omega_2^2}{c^2}\left[\frac{\omega_p^2}{\omega_2^2-\omega_c^2}\frac{\omega_c}{\omega_2}\right]\right]\left[k_{2x}^2-\frac{\omega_2^2}{c^2}\left[1-\frac{\omega_p^2}{\omega_2^2}\right]\right]\right.$$
$$-(\omega_0-\alpha\omega_c)\left\{\left[k_{2x}^2-\frac{\omega_2^2}{c^2}\left[1-\frac{\omega_p^2}{\omega_2^2}\right]\right]\left[k_{2z}^2-\frac{\omega_2^2}{c^2}\left[1-\frac{\omega_p^2}{\omega_2^2-\omega_c^2}\right]\right]-k_{2x}^2k_{2z}^2\right\}\Bigg]$$
$$\times\left[\frac{fk_x}{\omega_c^2+f^2}\left[\frac{\omega_2}{\omega_0}k_0-\frac{\omega_0-\alpha\omega_c}{\omega_2}k_{2x}-\frac{\omega_c(\omega_c-\alpha\omega_0)}{\omega_c^2-\omega_0^2}(k_0-k_{2x})\right]\right.$$
$$\left.-\frac{\omega_ck_x}{\omega_c^2+f^2}\left[\frac{\omega_c}{\omega_0}k_0+\frac{\omega_c(\omega_0-\alpha\omega_c)}{\omega_c^2-\omega_0^2}k_0+\frac{\omega_c^2(\omega_c-\alpha\omega_0)}{\omega_2(\omega_c^2-\omega_0^2)}k_{2x}\right]-\frac{i(\omega_0-\alpha\omega_c)}{\omega_2 f}k_zk_{2z}\right]$$
$$+k_{2x}k_{2z}\left\{(\omega_c-\alpha\omega_0)\left[k_2^2-\frac{\omega_2^2}{c^2}\left[1-\frac{\omega_p^2}{\omega_2^2-\omega_c^2}\right]\right]-(\omega_0-\alpha\omega_c)\left[\frac{\omega_2^2}{c^2}\left[\frac{\omega_p^2}{\omega_2^2-\omega_c^2}\frac{\omega_c}{\omega_2}\right]\right]\right\}$$
$$\times\left[\frac{i(\omega_c-\alpha\omega_0)}{f}\left[\frac{1}{\omega_2-k_2^2V_e^2/\omega_2}-\frac{1}{\omega_2}\right]k_zk_{2x}\right]\Bigg]\,, \tag{27}$$

$$|V_{0y}|=eE_{0y}/m(\omega_c-\omega_0)\,, \tag{28}$$

and $|\overleftrightarrow{D}_{1,2}|$ are the determinants of $\overleftrightarrow{D}_{1,2}$.

III. GROWTH RATES

When the resonance conditions

$$\omega_{1,2}=\omega\mp\omega_0\,,\qquad \vec{k}_{1,2}=\vec{k}\mp\vec{k}_0\,, \tag{29}$$

are satisfied, we can expand[16] ϵ and $|\overleftrightarrow{D}_{1,2}|$ as

$$\omega=\omega+i\gamma\,,$$
$$\epsilon\simeq i(\gamma+\gamma_L)(\partial\epsilon/\partial\omega)\,, \tag{30}$$
$$|\overleftrightarrow{D}_{1,2}|\simeq i(\gamma+\gamma_{L1,L2})(\partial|\overleftrightarrow{D}_{1,2}|/\partial\omega_{1,2})\,,$$

where γ is the growth rate for the process under investigation, and γ_L, γ_{L1}, and γ_{L2} are the damping rates of the low-frequency mode and the high-frequency scattered sidebands. We now neglect the linear damping of the decay waves. It may be mentioned here that one could write expressions for the linear damping rates of the decay waves by considering the effect of collisions in the corresponding dispersion relations of the decay waves. Thus, the growth rate γ_0 of the four-wave parametric process, in the absence of the linear damping of the decay waves, is given by

$$\gamma_0^2=-\frac{1}{\partial\epsilon/\partial\omega}\left[\frac{\mu_1}{\partial|\overleftrightarrow{D}_1|/\partial\omega_1}+\frac{\mu_2}{\partial|\overleftrightarrow{D}_2|/\partial\omega_2}\right]. \tag{31}$$

In the following we consider two special cases, viz., the filamentation and modulational instabilities of the incident upper hybrid laser radiation.

A. Filamentation instability

Here, we consider that the low-frequency electrostatic perturbation is due to the ion acoustic mode ($\omega=kC_s$, C_s is the ion sound speed) in the plasma and is propagating in the z direction, so that $k_x=0$ and $k_z=k$. Therefore, the undamped growth rate γ_0 of the filamentation instability is given by Eq. (31) where

$$\frac{\partial\epsilon}{\partial\omega}=\frac{2\omega\omega_p^2}{(\omega^2-k^2V_e^2)^2} \tag{32}$$

and

$$\frac{\partial|\overleftrightarrow{D}_{1,2}|}{\partial\omega_{1,2}}\simeq-\frac{2\omega_c^2\omega_{1,2}}{c^4}\left[\frac{\omega_p^2}{\omega_0^2-\omega_c^2}\right]^2\times\left[k_{1x,2x}^2-\frac{\omega_0^2}{c^2}\left[1-\frac{\omega_p^2}{\omega_0^2}\right]\right]. \tag{33}$$

We have calculated the growth rate of the filamentation instability for the following plasma parameters:

$$\omega_0=1.778\times10^{14}$$

in rad sec^{-1} (corresponding to CO_2-laser radiation);

$$\omega_c=10^{12}-10^{14},\quad \omega_p=(0.1-2)\times10^{14}\,,$$

both in rad sec^{-1};

$$V_e=2.6\times10^9$$

in cm sec^{-1} (corresponding to $T_e=4$ keV);

$$C_s=10^8$$

in cm sec^{-1};

$$k=10^2-10^3$$

in cm^{-1}; and

$$|V_{0y}/c|=10^{-4}\,.$$

The results of the calculation of γ_0 as functions of ω_p, ω_c, and k are displayed in the form of curves in Figs. 1, 2, and 3.

Figure 1 shows the variation of the undamped growth rate γ_0 as a function of the electron plasma frequency ω_p. It is seen that the growth rate decreases with increasing ω_p up to $\omega_p = 1.5\times 10^{14}$ rad sec^{-1}. The present theory is not valid beyond this value of ω_p.

Figure 2 shows the variation of the growth rate γ_0 as a function of the electron cyclotron frequency ω_c. The growth rate decreases with increasing ω_c up to $\omega_c = 5\times 10^{13}$ rad sec^{-1}. The present theory is not valid for $\omega_c > 5\times 10^{13}$ rad sec^{-1}.

Figure 3 shows the variation of the grwoth rate γ_0 of the filamentation instability as a function of the wave number k of the perturbation. The growth rate increases slowly, attains a maximum value, and then decrease gradually. It may be mentioned here that for large values of k, $b = k^2V_e^2/2\omega_c^2 \geq 1$. In this high-value regime of the wave number k the fluid theory breaks down and the Vlasov equation must be employed to find the nonlinear response of electrons.

B. Modulational instability

In this case we consider that the low-frequency electrostatic perturbation $(\omega, \vec{k})$ propagates along the direction of propagation of the incident laser beam (x axis), so that $k_x = k$ and $k_z = 0$. We calculate the growth rate γ_0 for the modulational instability, where $\partial \mid \overleftrightarrow{D}_{1,2} \mid / \partial\omega_{1,2}$ are given by Eqs. (33) and

$$\frac{\partial\epsilon}{\partial\omega} = \frac{2\omega\omega_p^2[\omega_c^2k^2V_e^2 + (\omega^2 - k^2V_e^2)^2]}{[\omega^2\omega_c^2 - (\omega^2 - k^2V_e^2)^2]^2} . \tag{34}$$

The values of ω for the calculation have been taken from the phase-matching condition that the phase velocity of the perturbation is equal to the group velocity of the incident laser radiation:

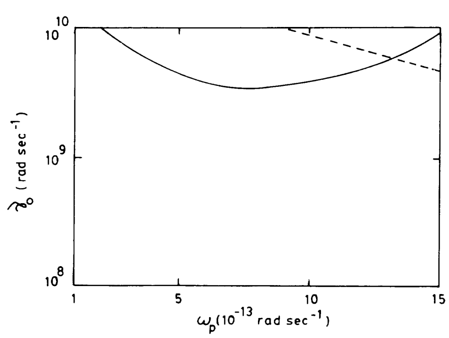

FIG. 1. Variation of the undamped growth rate γ_0 with the electron plasma frequency ω_p for the following parameters: $\omega_0 = 1.778\times 10^4$ rad sec^{-1}, $\omega_c = 1.75\times 10^{13}$ rad sec^{-1} ($B_s = 1$ MG), $V_e = 2.6\times 10^9$ cm sec^{-1} ($T_e = 4$ keV), $k = 10^2$ cm^{-1}, $C_s = 10^8$ cm sec^{-1}. Solid curve represents the modulational instability for $\mid V_{0y}/c \mid = 10^{-4}$ and the dashed curve represents the filamentation instability for $\mid V_{0y}/c \mid = 10^{-5}$.

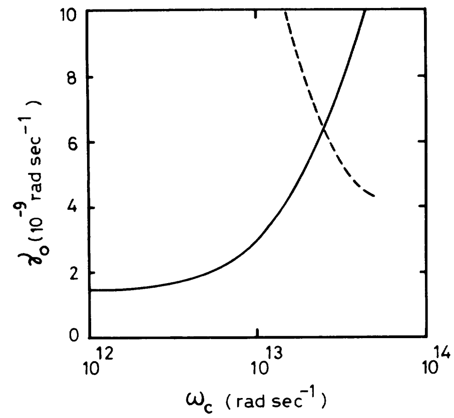

FIG. 2. Variation of γ_0 with ω_c. Solid curve represents the modulational instability for $\mid V_{0y}/c \mid = 10^{-4}$ and $\omega_p = \omega_0/4$, and the dashed curve represents the filamentation instability for $\mid V_{0y}/c \mid = 10^{-5}$ and $\omega_p = 0.85\omega_0$. Other parameters are the same as in Fig. 1.

$$\omega = kk_0c^2 \left[\omega_0 \left[1 + \frac{\omega_p^2\omega_c^2}{(\omega_0^2 - \omega_{UH}^2)^2} \right] \right]^{-1} . \tag{35}$$

The results of the calculations are also displayed in Figs. 1, 2, and 3. The variation of the growth rate with the electron plasma frequency ω_p is shown in Fig. 1. The growth rate decreases with increasing ω_p up to a certain value and then increases slowly with ω_p. It is noticed from Fig. 2 that the growth of the modulational instability increases with the faster growth rate at the higher magnetic field. The variation of the growth rate of the modulational instability as a function of the wave number of the perturbation is also shown in Fig. 3. It is observed that the growth rate is almost insensitive to the value of k.

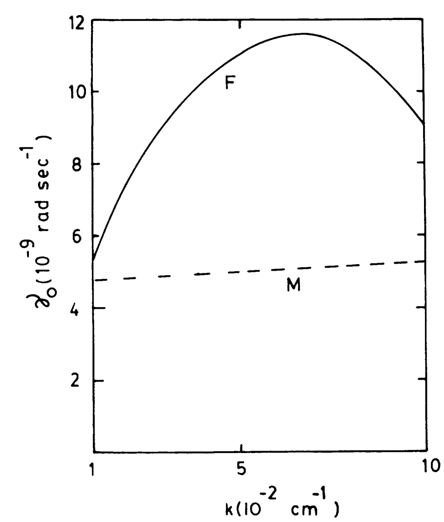

FIG. 3. Variation of γ_0 with k. Solid curve represents the filamentation instability for $\omega_p = 0.85\omega_0$, $\omega_c = 1.75\times 10^{13}$ rad sec^{-1}, and $\mid V_{0y}/c \mid = 10^{-5}$, while the dashed curve represents the modulational instability for $\omega_p = \omega_0/4$, $\omega_c = 1.75\times 10^{13}$ rad sec^{-1}, and $\mid V_{0y}/c \mid = 10^{-4}$. Other parameters are the same as in Fig. 1.

IV. DISCUSSION

A high-power laser radiation propagating transverse to the direction of the self-generated dc magnetic field of the order of a few megagauss is effectively unstable for the filamentation and modulational instabilities in a hot, collisionless and homogeneous plasma. For the following typical plasma parameters:

$$\omega_0 = 1.778\times 10^{14}$$

in rad sec^{-1} (corresponding to a CO_2 laser),

$$\omega_c = 1.75\times 10^{13}$$

in rad sec^{-1} (corresponding to $B_s = 1$ MG),

$$V_e = 2.6\times 10^{9}$$

in cm sec^{-1} (corresponding to $T_e = 4$ keV),

$$C_s = 10^{8}$$

in cm sec^{-1},

$$k = 10^{2}$$

in cm^{-1}, and

$$|V_{0y}/c| = 10^{-5}$$

(corresponding to the power density of the incident beam ~ 1 MW cm^{-2}), the growth rate of the filamentation instability turns out to be $\sim 10^9$ rad sec^{-1} and the growth rate of the modulational instability turns out to be $\sim 10^8$ rad sec^{-1}. It is also noticed that the growth rate decreases with increasing magnetic field in the case of filamentation instability, whereas the growth rate increases with increasing magnetic field in the case of the modulational instability.

By the choice of the perturbation we are restricting ourselves to the long-wavelength perturbations. For higher values of the wave number k of the perturbations, the fluid model of the plasma will break down. Again, the minimum value of k must also be such that the perturbation wavelength is less than the size of the laser fusion targets usually employed in the laser-target experiments.

It may be mentioned here that the effects of the inhomogeneity in the plasma and the saturation of the instabilities are also the problem of great importance.

ACKNOWLEDGMENT

The author is thankful to Professor M. A. Quader for his encouragement during the course of the work.

---

[1]J. A. Stamper, K. Papadopoulos, S. O. Dean, E. A. McLean, and J. M. Dawson, Phys. Rev. Lett. 26, 1012 (1972).

[2]J. A. Stamper and D. A. Tidman, Phys. Fluids 16, 2024 (1973).

[3]D. A. Tidman and R. A. Shanney, Phys. Fluids 17, 1207 (1974).

[4]J. A. Stamper and B. H. Ripin, Phys. Rev. Lett. 34, 138 (1975).

[5]J. J. Thomson, C. E. Max, and K. Estabrook, Phys. Rev. Lett. 35, 663 (1975).

[6]W. F. Divergilio, A. Y. Wong, H. C. Kim, and Y. C. Lee, Phys. Rev. Lett. 38, 541 (1977).

[7]B. Bezzerides, D. F. DuBois, D. W. Forslund, and E. L. Lindeman, Phys. Rev. Lett. 38, 495 (1977).

[8]T. Speziale and P. J. Catto, Phys. Fluids 21, 2063 (1978).

[9]Y. Sakagami, H. Kawakami, and S. Nagao, Phys. Rev. Lett. 42, 839 (1979).

[10]C. E. Max, W. Manheimer, and J. Thomson, Phys. Fluids 21, 128 (1978).

[11]W. M. Manheimer, C. E. Max, and J. Thomson, Phys. Fluids 21, 2009 (1978).

[12]M. N. Rosenbluth, Phys. Rev. Lett. 29, 565 (1972).

[13]M. N. Rosenbluth, R. B. White, and C. S. Liu, Phys. Rev. Lett. 31, 697 (1973).

[14]J. F. Drake and Y. C. Lee, Phys. Rev. Lett. 31, 1197 (1973).

[15]Y. C. Lee and P. K. Kaw, Phys. Fluids 15, 911 (1975).

[16]C. S. Liu and P. K. Kaw, in *Advances in Plasma Physics,* edited by A. Simon and W. B. Thompson (Wiley, New York, 1976), Vol. VI, p. 83.

[17]C. S. Liu, in Ref. 16, p. 121.

[18]N. Tzoar, Phys. Rev. 178, 356 (1969).

[19]J. Larson, Plasma Phys. 14, 467 (1975).

[20]P. K. Shukla, M. Y. Yu, and K. H. Spatschek, Z. Naturforsch. 30a, 911 (1975).

[21]S. Johnston and A. N. Kaufman, in Third Topical Conference on Radio Frequency Plasma Heating, Califronia Institute of Technology, January, 1978 (unpublished).

[22]V. K. Tripathi and R. R. Sharma, Phys. Fluids 22, 1799 (1979); C. Grebogi and C. S. Liu (private communication).

[23]M. Porkolab and M. V. Goldman, Phys. Fluids 19, 872 (1976).

[24]P. Kaw, G. Schmidt, and T. Wilcox, Phys. Fluids 16, 1522 (1973).

[25]J. Drake, P. K. Kaw, Y. C. Lee, G. Schmidt, C. S. Liu, and M. N. Rosenbluth, Phys. Fluids 17, 778 (1974).

[26]R. Bingham and C. N. Lashmore-Davies, Nucl. Fusion 16, 67 (1976).

[27]A. Ng, D. Salzmann, and A. A. Offenberger, Phys. Rev. Lett. 43, 1502 (1979).

[28]Md. Salimullah and Farida Majid, Phys. Rev. A 25, 555 (1982).

[29]Md. Salimullah and Tarsem Singh, J. Phys. Chem. Solids 43, 1087 (1982).

[30]M. S. Sodha, A. K. Ghatak, and V. K. Tripathi, Prog. Opt. 13, 169 (1976).